REVIEW

Antarctica in 2025: Drivers of deep uncertainty in projected ice loss

Helen Amanda Fricker[1]*, Benjamin K. Galton-Fenzi[2,3,4], Catherine Colello Walker[5], Bryony Isabella Diana Freer[1], Laurie Padman[6], Robert DeConto[7]

Antarctica is a vital component of Earth's climate system, influencing global sea level, ocean circulation, and planetary albedo. Major knowledge gaps in critical processes—spanning the atmosphere, ocean, ice sheets, underlying beds, ice shelves, and sea ice—create uncertainties in future projections, hindering climate adaptation and risk assessments of ice intervention strategies. Antarctica's ice sheet could contribute 28 centimeters to sea level by 2100, and potentially more if we surpass warming thresholds that trigger instabilities and rapid retreat. We review recent advances in understanding the changing stability of the ice sheet margins and identify key processes that require further research. Progress requires high-resolution satellite data, targeted field campaigns, improved modeling, and refined theory. Increased investment and interdisciplinary collaboration are essential to uncovering Antarctica's hidden processes and reducing uncertainties in future projections.

The Antarctic Ice Sheet (AIS) is Earth's largest freshwater reservoir, storing enough ice to add 58 m to global sea level if it all melted, with ~5.3 m from the West Antarctic Ice Sheet (WAIS) and the rest from the East Antarctic Ice Sheet (EAIS) (*1*). Other land ice reservoirs are the Greenland Ice Sheet (GrIS; 7.4 m) and glaciers and ice caps (GIC; 0.5 m). During the 20th century, global sea level rise (SLR) was dominated by ocean thermal expansion and GIC melt (*2*); however, over the past two decades, accelerated mass loss from GrIS and WAIS has made land ice (including GIC) the largest contribution [(*2*, *3*); Fig. 1A]. Between 1979 and 1989, the total AIS contribution was just 0.11 mm per year (*4*). In the early 1990s, AIS SLR contribution started to accelerate, reaching 0.19 mm per year for the period 1992 to 1996 and 0.32 mm per year for 2017 to 2020 (*3*). Models often do not capture the trends, leading to large differences between simulated and observed ice sheet changes. Projections initialized in 2016 indicate that most simulations produce a growing ice sheet over the ~5-year overlap period with observations, and this growth persists for several decades before eventual retreat occurs (Fig. 1B). This leads to diverging outcomes over time and greater uncertainty in long-term projections (*5*). Future AIS mass is so poorly known that the IPCC considers it "deeply uncertain" (*6*). The AIS could raise sea levels by 28 cm by 2100, equaling the contribution due to thermal expansion, and up to 6.9 m by 2300 under high emissions [(*6*); Fig. 1B], with uneven impacts globally (*7*). Flood risks are compounded by increased storminess from climate change, leading to the need for more complex adaptation strategies (*8*).

WAIS and EAIS have been identified as being vulnerable to crossing tipping points where abrupt, irrecoverable change occurs if a threshold in global average temperature is exceeded (*9*). The temperature threshold for WAIS is estimated at >1.5°C above preindustrial levels, which could occur by 2030 (*10*). Owing to its size, thickness, and location, EAIS is thought to be less sensitive, with a threshold of 4°C, based on response to past climate perturbations [(*11*); Fig. 2A]. These thresholds may be conservative, given that they are inferred from paleo warming rates that are much lower than those of today (*12*) and given the uncertainty in how globally averaged warming manifests in Antarctica. Projections of ice sheet tipping points are sensitive to where the models start from (initial conditions), the geometry of ice and the underlying bed, climate forcing, representation of the processes that control the change (*6*, *13*, *14*), and model numerics. Small variations in these inputs can lead to large differences in projected SLR. Determining the exact timing and magnitude at which tipping points are reached remains a huge challenge; therefore, AIS projections diverge widely in both the onset and magnitude of mass loss (*8*, *15*).

Uncertainty in future AIS mass loss stems from a limited understanding of physical processes that act at dynamic ice margins, which are missing or crudely represented in models (Fig. 2B), combined with uncertain future changes in climate forcing (*14*, *16*, *17*). These processes are undersampled because they occur on spatial and temporal scales and in locations beyond our present observational capabilities (see the scales of change in Fig. 2B) and involve complex feedbacks between the AIS, ice shelves, sea ice, seabed, ocean, and atmosphere (*2*, *18*), with insufficient observations (*19*, *20*). As more data

[1]Scripps Polar Center, IGPP, Scripps Institution of Oceanography, University of California, San Diego, La Jolla, CA, USA. [2]Australian Antarctic Division, Kingston, TAS, Australia. [3]Australian Antarctic Program Partnership (AAPP), Institute for Marine and Antarctic Studies, University of Tasmania, Hobart, TAS, Australia. [4]Australian Centre for Excellence in Antarctic Science (ACEAS), University of Tasmania, Hobart, TAS, Australia. [5]Department of Applied Ocean Physics and Engineering, Woods Hole Oceanographic Institution, Woods Hole, MA, USA. [6]Earth and Space Research, Corvallis, OR, USA. [7]Department of Earth, Geographic, and Climate Sciences, University of Massachusetts Amherst, Amherst, MA, USA.
*Corresponding author. Email: hafricker@ucsd.edu

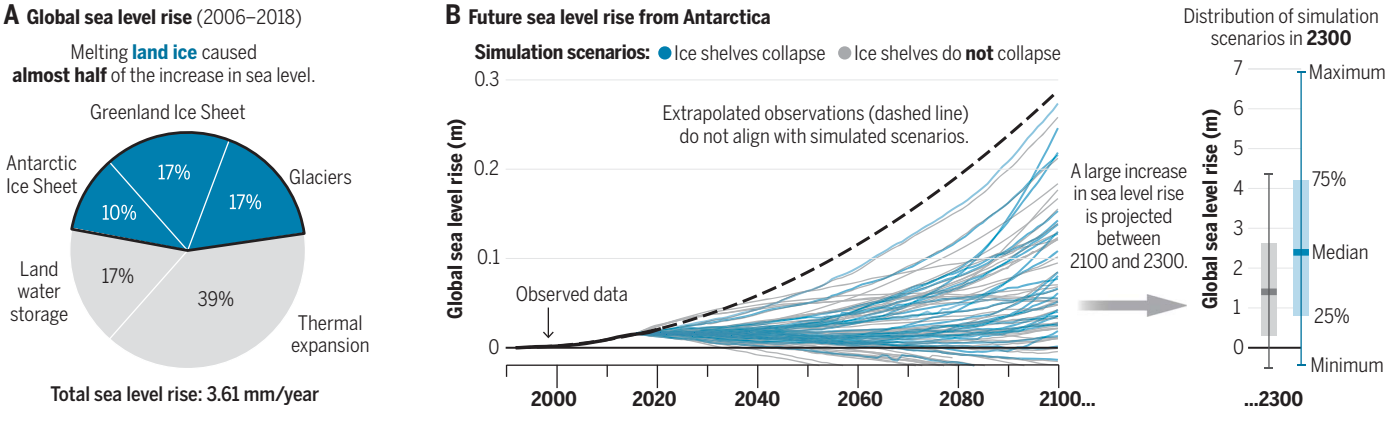

CREDIT: ADAPTED BY M. HERSHER/*SCIENCE*

Fig. 1. Antarctica as a dynamic freshwater reservoir. (**A**) AIS contribution to global SLR for 2006–2018 compared with contributions from other sources (*2*). (**B**) Observed AIS contribution to SLR for 1992–2020 (*201*) and projected future contribution to 2100 and 2300 (*5*), amid deep uncertainty (*6*).

are acquired at finer scales through new satellite missions and fieldwork, we are learning more about these processes, moving us closer to being able to represent them in models. In this Review, we summarize key pieces of the Antarctic system and the advances in our understanding of relevant processes, instabilities, and feedbacks since 2020, the epoch of the latest IPCC report (*21*). We highlight opportunities for impactful future research as we approach the Fifth International Polar Year (Box 1).

Pieces of the Antarctic system

Antarctica functions like a millennial-scale freshwater conveyor belt, accumulating snowfall that compacts into ice and returning melted freshwater to the ocean. At the same time, the AIS acts as a heat sink, slowing changes in the global heat content of Earth's atmosphere and oceans (*22*). Snowfall and ice accumulate gradually across the continent, with the total surface mass balance reaching ~2300 billion tonnes (or gigatonnes; Gt) per year (*23*). Being thicker in the interior, ice flows under the influence of gravity to the margins, where it forms floating ice shelves (Fig. 2B). Ice is then lost by iceberg calving and ocean-driven basal melting (Fig. 3), which pumps freshwater into the Southern Ocean either locally via meltwater plumes or away from the continent as icebergs melt. In steady state, the gains are balanced by losses at the margins. How climate warming will affect future snow accumulation is uncertain; however, there is a general consensus that losses around the edge of the continent will increase (*5*). Future AIS mass loss is contingent on how climate forcings evolve and how this triggers key processes around the margin.

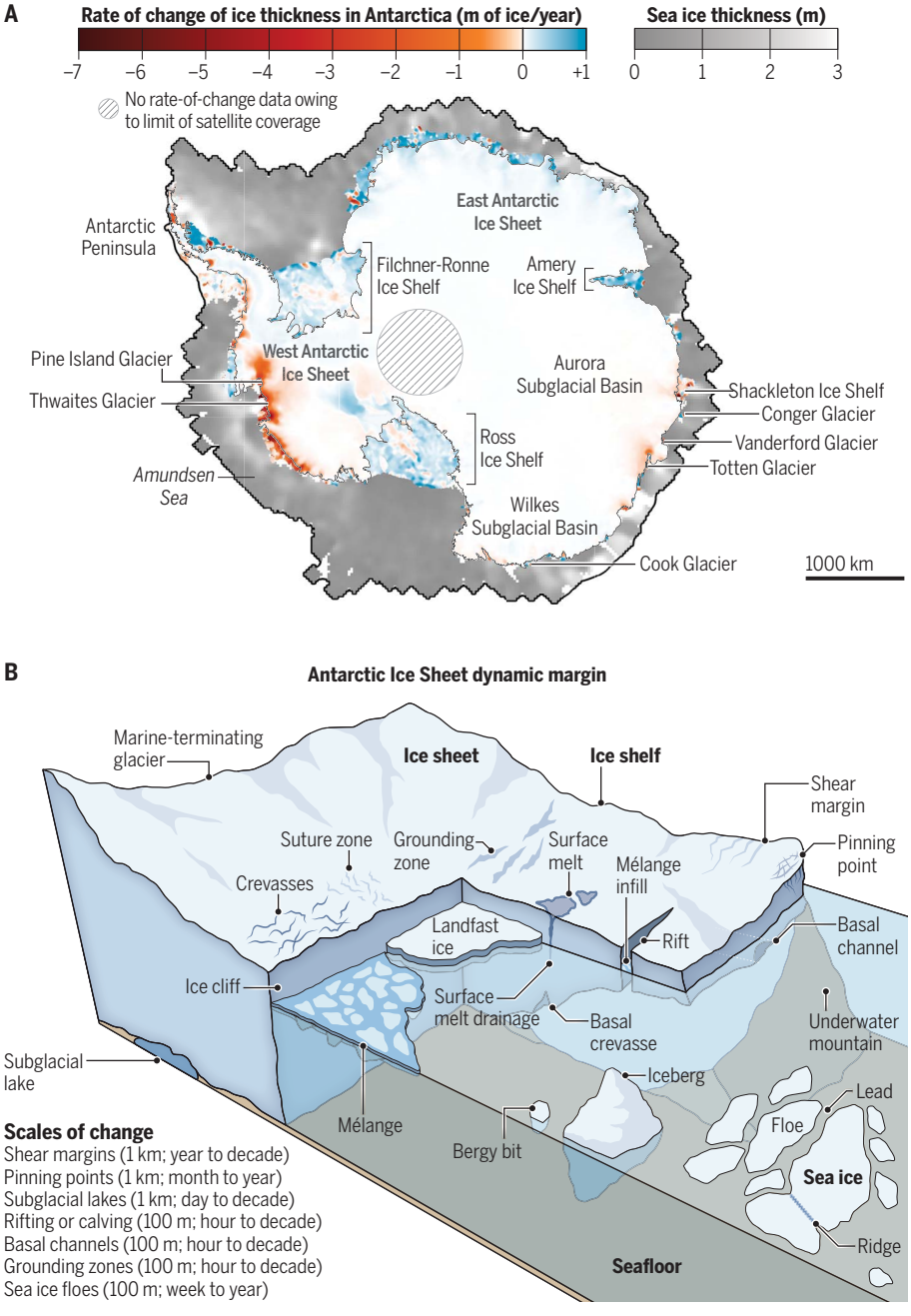

CREDIT: ADAPTED BY A. FISHER AND M. HERSHER/*SCIENCE*

Fig. 2. Antarctica's land ice and sea ice. (**A**) AIS thickness changes for 2003–2019 from Ice Cloud and land Elevation Satellite (ICESat) and ICESat-2 satellite laser altimetry (*48*) as well as sea ice thickness for January 2020 from ICESat-2 (*111*) [from (*203*)]. [Credit: Modified from (*48*), (*202*), and (*111*) CC BY 4.0] (**B**) Features associated with processes acting in AIS's dynamic ice margins on a range of spatial and temporal scales (table at bottom left).

Antarctica's subglacial system is a basal lubricant

The speed of AIS ice flow is influenced by basal conditions that determine how easily ice slides over the bed owing to the presence of liquid water and bed deformability. Fastest ice flow tends to occur where pressurized water is present at the base (*24*). Subglacial water is generated as ice melts from frictional heat caused by the glacier flow, geothermal heat flux, and pressure melting (*25*). Basal meltwater production rates are low (millimeters per year) but, over the vast AIS, the volume is substantial [59 Gt per year; (*26*)]. The AIS subglacial system is largely insulated from climate; by contrast, in Greenland the surface meltwater can reach the bed to drive a seasonal ice flow cycle (*27*). Observations of seasonal signals have only recently emerged on the Antarctic Peninsula, which are primarily attributed to seasonal modulation of ice-ocean-atmosphere interactions, with particular sensitivity to glacier terminus change, ocean temperatures, and surface water availability that may penetrate to the bed (*28*, *29*). Elsewhere, AIS surface melt is mostly confined to ice shelves (*30*, *31*), but if it were to migrate above the grounding line (GL; Fig. 3) and then reach the bed, some AIS outlets could evolve toward more seasonally varying flow speeds and accelerated ice loss [for example, see (*32*)].

Subglacial hydrology is rarely observed, and so it is either crudely represented in or missing from models [for example, see (*33*)]. Our observational capability was transformed in the mid-2000s by the realization that fluctuations in local surface elevation are signatures of subglacial hydrology (*34*, *35*), with satellite laser altimetry tallying >140 interconnected subglacial lakes that are continuously filling and draining (*36*). Localized ice flow acceleration has been observed during periods of subglacial lake drainage (*37*–*39*), but the impact on wider ice sheet dynamics remains poorly sampled (*40*). Subglacial water follows the hydropotential,

Box 1. Bridging the gaps in SLR projections.

The wide range of present Antarctic SLR projections is too broad for policy-makers to use effectively. Improving these projections requires a better understanding of mass balance processes, especially those occurring on short spatial (~100 m to ~1 km) and temporal (daily to seasonal) scales, which are presently underrepresented in models because observations have been insufficient in space and time.

Main knowledge gaps

To reduce uncertainties in Antarctic mass loss and better inform policy decisions and adaptation strategies, we must advance knowledge of the following:
- Subglacial hydrology, basal processes, and internal ice deformation and structure
- Ice sheet geometry and the potential for MISI
- GZ state and variability and the role of buttressing
- Sub–ice shelf cavity melting, ocean circulation, and ice-ocean interactions
- Fracturing and calving dynamics and the potential for MICI
- Feedbacks between the ice sheet, sea ice, and other parts of the climate system
- Interactions between global climate and regional climate at the ice sheet margin, including accumulation and surface warming

These knowledge gaps require mapping of the seabed and bedrock underlying the ice sheet, determination of the properties under the grounded ice and floating ice shelves, enhanced simulation and modeling, and stronger interdisciplinary and multinational research to investigate feedbacks.

Essential actions

- Advance understanding of processes by monitoring relevant variables across a range of space and time scales with airborne and satellite missions that ensure continuity and innovation through high-resolution, frequent sampling: Key future missions include the NASA–ISRO Synthetic Aperture Radar (NISAR) mission (ice velocity and deformation), the European Space Agency's Copernicus Polar Ice and Snow Topography Altimeter (CRISTAL) mission (surface elevation), and the proposed Earth Dynamics Geodetic Explorer (EDGE) mission (surface elevation)
- Perform targeted field observations for evaluation and calibration of remote-sensing techniques and to develop field-based understanding of processes
- Expand field observations beyond WAIS, particularly to at-risk EAIS outlet glaciers and ice shelves
- Develop high-fidelity simulations that exploit progress in closing the main knowledge gaps and the reproduction of observed changes for future projections with substantially reduced uncertainties, for example, Ice Sheet Modeling Intercomparison for the seventh IPCC Ice Sheet Model Intercomparison Project for Coupled Model Intercomparison Project–Phase 7 (ISMIP7)
- Educate and inspire the next generation of Antarctic ice sheet researchers
- Provide actionable projections with well-constrained uncertainties that inform policy decisions and adaptation strategies

Funding and advocacy

Strong advocacy for Antarctic research is crucial to secure sustained funding and refine projections, which are essential for guiding climate policies and global adaptation strategies. This requires enhanced coordination among scientific, governmental, public, and private stakeholders, as well as increased international collaboration [e.g., coordinated through the Climate and Cryosphere (CLiC) project and the Scientific Committee on Antarctic Research's INStabilities & Thresholds in ANTarctica (SCAR INSTANT) research program].

and, in some regions, subtle thickness changes may divert water from one drainage basin to another (*41*). Evidence of a deep groundwater network beneath a WAIS ice stream (*42*) indicates another source for subglacial water. It has been hypothesized that this groundwater interaction may be crucial on decadal timescales (*43*). Identifying the sources, thickness, and pressure of subglacial water beneath the ice sheet will be critical for understanding its present and future controls on ice dynamics (*44*, *45*).

Antarctica's ice shelves are buttressing dams

Most AIS outlet glaciers presently terminate in ice shelves. Ice shelf contact with pinning points (where the ice base touches seabed highs) and lateral shear margins (where ice is in contact with rock or slow-moving ice) leads to buttressing of upstream ice (*46*). Each basin experiences drivers of change on different timescales (Fig. 3), giving each ice shelf a unique ratio of mass loss processes. If mass losses exceed gains, then the ice shelf thins and/or the GL retreats, resulting in reduced basal friction, less drag at pinning points and sidewalls, and less buttressing (*46*, *47*). As a result, more ice discharges to the ocean, increasing SLR. Regions where the grounded AIS is losing the most mass are those where ice shelves are thinning (*48*). Hence, although the net loss of grounded ice determines SLR, understanding the role of floating ice is crucial to predict change.

Ice shelf thinning can trigger faster ice flow hundreds of kilometers away (*46*, *49*) and can be especially impactful if it occurs upstream of a stable "safety zone" (*47*) or causes the ice to detach from pinning points (*50*, *51*). Buttressing can be lost through thinning, unpinning, and complete ice shelf disintegration, a phenomenon that involves a series of interconnected processes such as enhanced calving (*52*, *53*), increased basal melting leading to ice shelf thinning (*54*, *55*), and, as observed on the Antarctic Peninsula, "hydrofracture" that results from excessive surface melt [(*56*); Fig. 3A].

Antarctica's sub-ice cavities are the hidden link to the ocean

Sub-ice cavities host a distinctive ocean environment where externally driven circulation of heat and salt couples with buoyant glacial meltwater generated by basal melting. Key factors that influence basal melt rates include ice depth and basal slope as well as seabed geometry (*57*, *58*). Ice shelves are often classified as cold or warm cavity, with distinct modes of melting and circulation (Fig. 3B). In reality, multiple modes and combinations of oceanic conditions can influence a single ice shelf at different times and locations (*57*, *59*). In warm cavities such as in the Amundsen Sea, Circumpolar Deep Water can exceed the local freezing point temperature by 2°C (*60*, *61*), with models suggesting that it would take 3 years to travel to the GL (*62*), where it drives melt rates of 10 to 100 m per year (*63*). In cold cavities, such as the Amery Ice Shelf, melt rates near the deep GL (Fig. 3B) are highest because the in situ freezing point temperature decreases with pressure (*64*). The resulting cold Ice Shelf Water can refreeze as marine ice at shallow ice drafts, redistributing ice (*57*, *59*, *63*) and stabilizing ice shelves (*65*). In both cavity types, rapid melting can occur at the ice fronts because of more energetic oceanic conditions as well as warmer upper-ocean waters in summer (*66*, *67*).

Future changes in Southern Ocean temperature, circulation, and sea ice conditions could shift the distribution of basal melting and refreezing (*68*). The complex interplay between buoyant intrusions of subglacial meltwater (*69*), ice-base geometry (*58*), and turbulent processes near the ice-ocean boundary leads to the emergence of several other melting and freezing regimes that are understudied (*59*, *70*). Substantially improved knowledge of the ice shelf cavity environment, including bed geometry, ocean

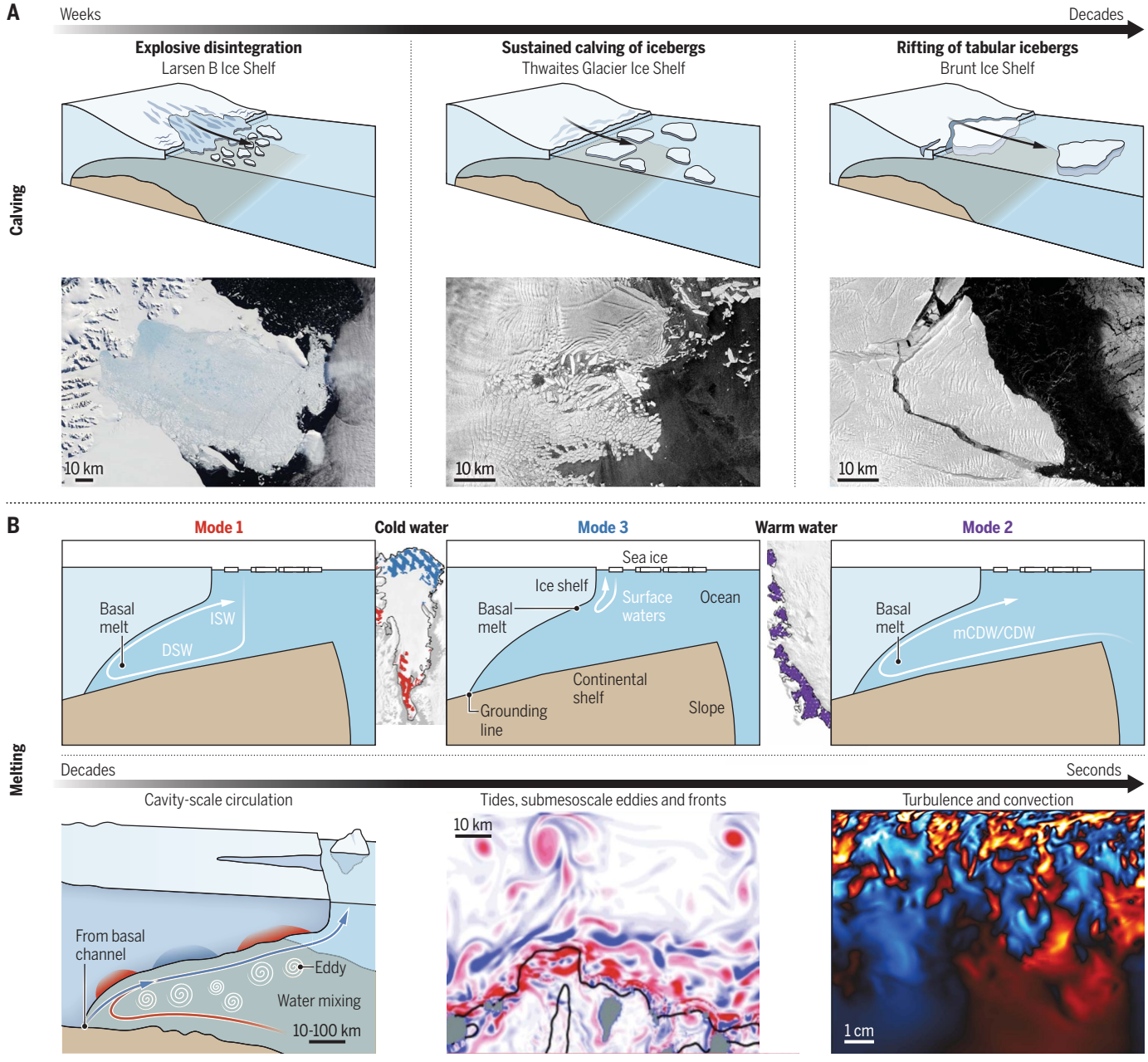

Fig. 3. Antarctica's mass loss processes and their spatial and temporal scales. (**A**) Calving is an irregular process where ice breaks off from outlet glaciers and ice shelves, ranging from large tabular icebergs calved every few decades, to more frequent smaller icebergs, to complete disintegration (*130*). [Credit: Modified from (*130*)] (**B**) Basal melting is a continuous process driven largely by cavity-scale circulation controlled by the cavity geometry (including the ice draft and slope, and the seabed shape) and by long-term changes in ocean conditions seaward of the ice front; mesoscale processes (such as eddies, fronts, and tides) that control how the ocean heat enters the cavity; and smaller-scale processes (such as turbulence and convection) (*57*, *59*). [Credit: Modified from (*59*) (bottom left), (*204*) CC BY 3.0 (bottom middle), and (*59*) (bottom right)] CDW, Circumpolar Deep Water; DSW, Dense Shelf Water; mCDW, modified Circumpolar Deep Water.

circulation, and mass loss processes, is needed to reduce uncertainties in projections of ice shelf mass loss (see Box 1).

Antarctica's grounding zones are complex intertidal estuaries

Antarctic ice first meets the sub–ice shelf cavity at the GL, which can migrate with ocean tides to create a grounding zone (GZ; Fig. 4), where the ice transitions from being always grounded to always floating. Ice flowing across the GL typically thins rapidly, as a result of stretching as basal friction is removed and high basal melt rates (*63*). Underwater surveys have revealed that basal melt close to the GL varies down to submeter scales as a result of local variations in basal ice topography (*61*). Autonomous phase-sensitive radio echo sounding (ApRES) instruments have revolutionized the measurement of basal melt rates; however, these techniques are difficult to apply in flexure zones, regions of crevassing, or where firn compaction rates and vertical shear profiles are difficult to determine (*71*–*73*). ApRES-derived estimates of melt rates can be combined with estimates from satellite-derived ice thickness changes (*63*); however, these are undersampled in the GZ owing to complex surface topography

and the breakdown of hydrostatic equilibrium (*74*), creating an observation gap in regions where melt rates are the highest.

Recent studies have shown that seawater intrusions driven by ocean tides can penetrate the GZ (Fig. 4), causing variations in basal melt on short timescales (*75*). Satellite-based radar interferometry (*76*–*78*) and laser altimetry observations (*79*) with high spatial resolution and frequent temporal sampling reveal that the GL can migrate up to 15 km between low and high tide, pumping relatively warm, salty ocean water further beneath the ice sheet every few hours (*80*). Significant long-term GL retreat and acceleration in Amundsen Sea glaciers has been attributed to vigorous ice-ocean interactions in their GZs (*75*, *81*).

Evidence is also emerging of a link between subglacial hydrology and ice shelf basal melting (Fig. 4). Injection of freshwater across the GZ into the ice cavity can enhance melting that reduces ice shelf buttressing, which has been proposed as an important mechanism for some EAIS glaciers (*69*, *82*). Models suggest that under high greenhouse gas emissions, this effect can increase the SLR contribution of a drainage basin by up to 30% (*83*). Focused discharge of subglacial freshwater across the GL can drive the development of large basal channels that mechanically weaken the ice shelf (*75*). Some studies have observed tens of kilometers of migration of seawater underneath the ice sheet, along estuaries formed by subglacial hydrology in the GZ, where water can be trapped for weeks before draining (*77*, *80*). Some models predict that the density difference between fresh subglacial discharge and salty ocean water can form a "salt wedge" that permits the diffusion of seawater up to several kilometers upstream of the GZ (*84*, *85*). This layered seawater intrusion theory—distinct from, yet potentially occurring alongside, the tidal intrusion mechanism—remains unobserved in Antarctica with present observational capabilities. Such irregular, widespread interactions between ice and seawater in the GZ could be impactful on AIS evolution (*85*–*87*), potentially doubling future SLR contributions (*88*); there is also a suggestion that this may introduce new tipping-point behaviors (*89*, *90*). Explicit representations of these GZ melt processes are missing from most ice sheet models (*80*).

Another GZ interaction involves sediment transfer from the ice sheet to the ocean, which can influence the stability of the GZ (*91*, *92*) (Fig. 4). Depositional features can also give insights into present and past ice dynamics; for example, more than 75 "GZ wedges" have been identified on the Antarctic seafloor, which form as sediment is delivered to the GZ during periods where the ice margin remains stable for a long time (*93*). GZ wedges, which are typically <15 km long and 15 to 100 m thick, can act as topographic pinning points that can stabilize the GL, with evidence that they halted WAIS retreat for hundreds to thousands of years during the last deglaciation (*94*). Smaller amplitude, regularly spaced corrugation ridges observed offshore of Thwaites Glacier and Larsen Inlet are thought to record sequential low-tide seafloor sediment imprints that may provide evidence of rapid GL retreat of hundreds of meters per day during the last deglaciation (*95*, *96*). Similar features in Pine Island Bay have been interpreted as the imprint of icebergs dragging on the seafloor at tidal frequencies (*97*). Although there are few direct observations, understanding feedbacks between ice dynamics and sediment redistribution in GZs is essential for interpreting their past stability and projecting future ice sheet retreat.

Antarctica's sea ice regulates global climate and ice sheet change

Antarctica's surrounding sea ice (Fig. 2A) covers an area of ~18.5×10^6 km^2 (~6% of the global ocean) at its winter maximum (September) and shrinks to nearly 16% of that in summer (*98*). Sea ice is a dynamic, seasonally varying component of the Antarctic environment, exerting a strong influence on the ocean and climate (*17*). Sea ice increases Earth's albedo, reflecting incoming solar radiation, and helps to regulate global temperature (*99*). The seasonal formation and melt of sea ice modifies ocean salinity and temperature, altering stratification and circulation patterns that govern the distribution of heat along the continental shelf, shaped by regional weather patterns and climate feedbacks (*100*). These processes determine where and how relatively warm waters can melt ice shelves, which can influence ice shelf stability and future sea level rise [for example, see (*101*, *102*)]. In turn, changes in ice shelf melting can affect sea ice, generating complex climate feedbacks (*103*). Sea ice also plays a crucial role in marine ecosystem activity (*104*).

A significant and unpredicted decline in Antarctic sea ice extent began in 2016, with partial recovery in 2019 to 2020 followed by consecutive years of near-historic lows (*105*), leading to increased coastal exposure to open water (*106*). The lowest annual sea ice extent was 1.79×10^6 km^2 in February 2023, which is ~10% less than the 2022 record low that marked the first time annual minimum extent dropped below 2×10^6 km^2 (*107*). The ongoing decline signals a major shift in Southern Ocean conditions (*105*), which has implications for sea ice and its influence on the AIS, the broader climate system (*108*, *109*) and ecosystems (*110*). Sea ice thickness—a key factor for ice strength, landfast ice formation, and summer survival—is challenging to measure in Antarctica because of thick snow cover, flooding, and difficulty in resolving leads to provide relative freeboard assessments (*111*). Accurately mapping sea ice freeboard and structure at scales that capture most sea ice floes (Fig. 2B) is essential for providing the detailed data needed to improve models of sea ice evolution (*112*) and explain why change has occurred.

Instabilities and feedbacks of the Antarctic system

Geometric instabilities at dynamic ice margins

Simple relationships predict the potential for two geometry-based high-end retreat scenarios, which are considered to be possible AIS instabilities: the marine ice sheet instability (MISI) and the marine ice cliff instability (MICI). MISI is based on the understanding that because seaward ice flux increases with ice thickness, GLs located on retrograde bed slopes are inherently unstable (*113*, *114*). In such locations, the weakening or loss of ice shelf buttressing can trigger a self-sustaining drawdown at the ice margins: Initial thinning causes the GL to retreat into deeper water, where a higher strain rate increases mass loss from the ice sheet, leading to further retreat and thinning. Although some studies suggest that MISI is underway in WAIS (*81*, *115*), others suggest that present-day GL retreat is driven by external climate forcing alone (*116*), though continued warming may eventually lead to MISI onset (*117*). Some EAIS outlets are also potentially vulnerable to MISI (*118*, *119*). MICI is predicated on simple force balance arguments that suggest that the stable height to which a marine-terminating ice cliff (Fig. 2B) can grow is limited by ice strength to ~100 m (*120*). If triggered, unstable cliff failure can repeatedly expose thicker ice upstream, driving rapid ice loss at the margin (*121*). As proposed, MICI could contribute multimeter SLR on century timescales (*2*).

MICI remains controversial and has not been directly observed in Antarctica, although observations of speed-up and enhanced calving at thick marine-terminating glaciers after ice shelf loss have been noted at Crane Glacier on the Antarctic Peninsula (*122*) and in Greenland (*123*). Paleo records of iceberg plow ridges in Pine Island Bay (*124*), previously attributed to grounding of floating ice during breakup (*97*), have been cited as indirect evidence for MICI. By contrast, a statistical analysis of modeling uncertainties (*125*) concluded that MICI is not required to reproduce sea level estimates in the geologic past. Process-based modeling suggests that slow ice shelf loss can mitigate MICI, but outcomes vary widely depending on assumptions of ice properties and ice strength (*126*). Other models suggest that speed-up and dynamic thinning of unbuttressed ice fronts can suppress ice cliff calving in the absence of ice shelves (*127*, *128*). An incomplete understanding of the material properties (strength) of glacial ice and the processes involved in triggering and amplifying ice shelf loss, calving, and cliff retreat (*129*, *130*) continues to make the role of MICI in retreat scenarios difficult to parameterize and quantify (*131*, *132*). Given the potential for MICI (and fracture and calving processes in general) to contribute to future ice loss, rifting and calving at thick ice margins should be further evaluated through observations at spatial and temporal scales relevant to processes involved in ice shelf, glacier, and ice front stability. Further research on the initiation and propagation of fracturing, the

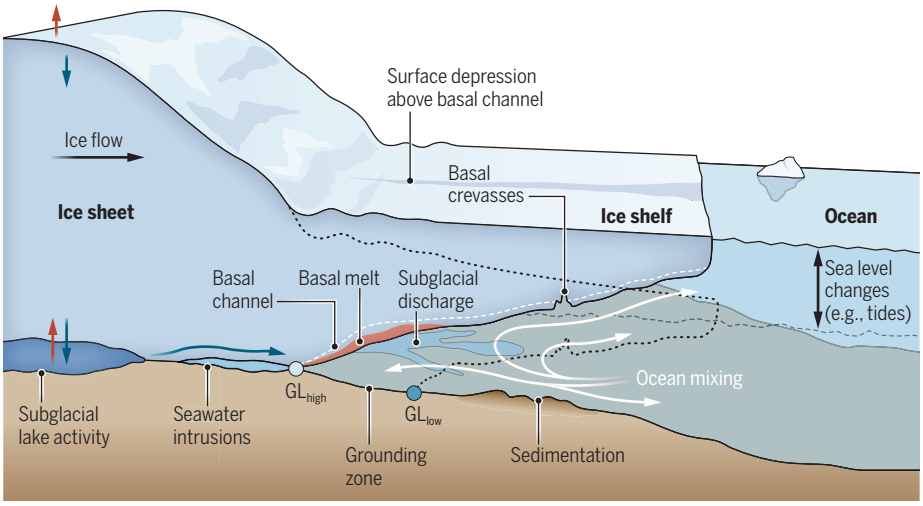

Fig. 4. Antarctica's grounding zones. Changes in ocean sea level, including from tides, can move the GL by up to several kilometers across the GZ (from GL_{low} to GL_{high}). Processes acting in and around the GZ—driven by interactions between ice, bedrock, sediment, subglacial hydrology, and the ocean—can vary on short spatial and temporal scales. Tides can pump relatively warm seawater kilometers inland, enhancing basal melting in and upstream of the GZ. Subglacial water flux from the ice sheet bed to the ocean across the GL can also enhance basal melting in the GZ, which can lead to the development of basal channels that are visible in satellite altimetry as surface depressions. Sediment flux into the sub–ice shelf cavity can increase GL stability. All of these interactions can influence long-term ice dynamics. Figure is not to scale.

role of GL location and floating versus grounded ice, upstream ice thickness gradients, surface melt, bedrock shape, and flow velocities is needed.

Feedbacks at dynamic ice sheet margins

Processes at AIS dynamic margins are interconnected and can compound. For example, ice front retreat due to increased iceberg calving can increase ocean heat supply to the deep GL (*133*, *134*). Enhanced basal melting leads to ice shelf thinning and the incision of basal channels (*135*), leaving ice shelves more susceptible to hydrofracture (*136*). Processes acting in certain locations, such as basal melting or rifting along shear margins or pinning points, can have a disproportionate impact, triggering rapid ice shelf retreat and flow acceleration (*137*, *138*). This can potentially lead to more crevassing, rifting, and ice front retreat. Such feedbacks have been implicated in the ongoing retreat and acceleration of Pine Island Glacier (*53*, *139*).

Not all feedbacks at ice sheet margins are positive. For example, ice sheet models accounting for glacial-isostatic adjustment, including the gravitational, rotational, and deformational response of a viscoelastic Earth to changing ice loads (*140*), demonstrate that bedrock uplift and a local sea level drop in the vicinity of retreating GZs can slow retreat. The effect is strongest in West Antarctica, where the mantle has relatively low viscosity (*141*), allowing for faster uplift rates. This negative feedback could slow both MISI- and MICI-driven retreat, although it will weaken as the pace of AIS ice loss increases.

Feedbacks between coastal processes and the AIS

The configuration of the coastal icescape (sea ice, fast ice, and icebergs) affects mass-loss processes (Fig. 3) through modification of ocean properties (*142*). Sea ice may enhance buttressing (*106*, *143*), mitigate the impacts of swells (*144*, *145*) and tsunamis (*146*, *147*) on ice fracture, and reduce frontal melting and small-scale calving (*148*, *149*). This role is amplified when thick landfast sea ice forms, anchored by complex coastlines and grounded icebergs (*150*), which affects polynya activity, associated abyssal ventilation, and the properties of water masses entering the cavity (*151*). Large calving events can greatly reduce polynya activity and the production of dense water that ventilates the abyssal global oceans (*152*). Poorly constrained calving models, limited water depth data, and complex sea ice physics hinder projections of changes in the coastal icescape.

AIS response to large-scale climate variability

Climate variability modes like the Southern Annular Mode and El Niño–Southern Oscillation influence ocean properties on the continental shelf (*153*), sea ice extent (*154*), and ice sheet/shelf surface mass accumulation (*155*), affecting the changing mass balance of WAIS ice shelves (*156*) and the grounded AIS (*157*). Modeling studies project that some cold-cavity ice shelves could transition to warm cavities by 2100 (*158*, *159*), caused in part by feedbacks as initial inflows of warm ocean waters drive melting that intensifies the cavity overturning circulation, continuing to draw in warmer water. However, these transitions may be delayed because an initial response to climate warming can involve a weakened sub-ice circulation and lowered basal melt rates (*160*).

Keeping track of the pieces of the Antarctic system

Antarctica's size and remoteness mean that changes on a continental scale can be tracked only by satellite. Three complementary techniques track grounded AIS mass: gravimetry; mass fluxes from ice flow rates, ice thickness, and climate models; and elevation changes combined with a firn density model. These techniques can then be combined (*3*). The net AIS mass budget is shaped by snow accumulation and seaward ice flow, influenced by complex interactions among the atmosphere, ocean, and ice (*48*), which occur on multiple scales. Therefore, comprehensive monitoring should span broad spatial and temporal scales, resolving features such as outlet glaciers (*28*, *161*) and ice shelves (*63*) while also capturing seasonal to annual changes. Only three studies have provided a comprehensive assessment of grounded and floating ice using the same data over the same time period (*48*, *162*, *163*) (Fig. 2A). Observations at higher spatial and temporal resolution can inform about processes not yet captured in models.

Broad-scale monitoring

Between 1992 and 2020, AIS experienced an overall net mass loss of grounded ice (*3*), dominated by trends in WAIS (82 ± 9 Gt per year) and the Antarctic Peninsula (13 ± 5 Gt per year). Most WAIS changes occur in the Amundsen Sea basins, where glaciers have accelerated because of reduced ice shelf buttressing and GL retreat (*46*, *48*, *54*). EAIS is near steady state or in slightly positive balance because losses from increased ocean-driven melt are offset by gains from increased inland snowfall, which is attributed to a warming and more moisture-laden atmosphere (*3*, *48*). Between 2003 and 2018, mass gains were concentrated in Queen Maud Land, whereas mass loss occurred in several MISI-susceptible ice outlets draining the Aurora and Wilkes subglacial basins (*48*), accompanied by GL retreat (*164*). Flow rates have increased in numerous EAIS outlets on both grounded ice [e.g., Cook Glacier (*165*) and Vanderford Glacier (*166*)] and floating ice [e.g., ice shelves of Scott Glacier (*167*), Totten Glacier (*168*), and Denman Glacier (*169*)].

Snow accumulation across AIS increased significantly between 2019 and 2023 (*170*). In WAIS, much of the mass gain was due to short-period extreme events, such as atmospheric rivers (ARs) (*170*–*172*). In 2019 to 2020 alone, this reduced WAIS's SLR contribution by 60 ± 16 Gt per year (*170*). Record mass gains occurred in 2022 (*173*), primarily because of an increase in precipitation events over EAIS, including ARs. In March 2022, a powerful 3-day AR delivered an estimated

306 Gt of precipitation (*174*), accounting for 32% of the total AIS precipitation for that month, and up to 90% in some parts of EAIS, particularly Wilkes Land. AR intensity may be linked to interannual climate modes, but both the intensity and frequency of extreme precipitation events are expected to rise as the climate warms throughout the 21st century (*172*). An open question is whether increased snowfall in the AIS interior will be sufficient to offset increased melting and calving at the margins.

Process-based understanding

Recent satellite data show changes on process-relevant spatial and temporal scales. In WAIS, Pine Island Glacier Ice Shelf transitioned in 2015 from a previously quasi-stable cycle of advance and retreat at its calving front to a calving regime characterized by more frequent calving of tabular icebergs (Fig. 3B) and calving front retreat (*175*) (Fig. 3B). Portions of the Thwaites ice tongue underwent an abrupt change from a previously intact ice shelf into fragmented remnants (*176*, *177*). Studies of ice shelf rifts have suggested that their activity may relate to internal formation mechanics (*178*) and glaciological stresses as well as to atmospheric and oceanic forcings, for example, winds (*179*), sea surface slope or wave swell (*180*, *181*) and tsunamis (*147*), ocean circulation (*61*), and strength of intrarift mélange (*182*). Observations of ice shelves with short calving cycles (Fig. 3A) have shown that ocean and atmospheric forcings can lead to ungrounding from pinning points, driving increased calving rates, for example, at Pine Island Glacier around 2006 (*133*), Thwaites Glacier (*183*), and Thwaites Eastern Ice Shelf (*177*, *184*). At Thwaites, the evolving interaction with a pinning point after the loss of Thwaites Western Ice Tongue in 2008 likely triggered shearing and fracture propagation related to enhanced weakening (*137*, *178*, *185*), with another ungrounding anticipated within the next decade (*50*).

In East Antarctica, there have been many signs of change, for example, recent terminus change after sea ice breakout (*186*) and GL retreat (*166*, *187*), but the first observed ice shelf disappearance was Conger-Glenzer in 2022 (*55*), after decades of retreat that began in the late 1990s when small calving events isolated it from Shackleton Ice Shelf. This was followed by phases of retreat, relative stability, and ultimate rapid disintegration driven by long-term thinning, reduced buttressing effect, and ungrounding from a pinning point. The evolution of the Shackleton-Denman system itself involved structural changes in the floating shear margins, rift propagation, and small-scale calving (*167*), possibly aided by seawater infiltration in some regions adjacent to Shackleton Ice Shelf (*164*, *188*) that may affect ice rheology (*189*). These could all be early signs of EAIS responding to warming.

Antarctica as a target for "ice intervention" to mitigate sea level rise

Intervention to slow ice loss has recently been suggested (*190*, *191*), with two primary strategies. Underwater curtains would divert warm water from reaching the ice outlets and redirect colder water toward them instead, potentially slowing ice melt and GZ retreat (*192*). Whether this will actually slow overall AIS mass loss is uncertain (*193*); it might simply reroute warm water to other ice shelves (*194*). Drilling and drying strategies aim to stabilize glaciers by increasing basal friction of sliding ice streams by drilling deep holes and removing lubricating water from the subglacial drainage system. This idea is based on observations of natural processes at Kamb Ice Stream. However, most outlets differ markedly from Kamb, and the actual impact on glacier sliding is expected to be highly dependent on poorly mapped and modeled bed and basal conditions. Because subglacial water is constantly replenished and may be connected to underlying groundwater (*42*), any impact would be short-term, and any efforts would need to be sustained.

Geoengineering in Antarctica faces immense challenges owing to its vast scale, technical and logistical difficulties, harsh polar conditions, and environmental concerns, including impacts on marine life and the risk of contaminating subglacial areas (*195*). Perhaps the greatest risk, however, lies in unintended consequences from our limited understanding of how ice sheets respond to climate and human activities. With the guiding principle of "first, do no harm," it is crucial that we prioritize improving our knowledge. This will help us better assess our options for the future and make informed decisions about what actions we can responsibly take. Effective methods will necessitate substantial, long-term investments in research, infrastructure, and ongoing monitoring—resources that would be more wisely allocated to addressing the fundamental deep uncertainties instead (*195*).

Commitment to change

The AIS is expected to continue losing ice in response to the heat already absorbed by the climate system (*196*). To date, only a small fraction of this global heat imbalance has contributed to AIS melting (*22*, *163*). Increased melt rates for WAIS may be committed for the next century (*197*). The pace and extent of AIS evolution are uncertain (*198*, *199*), influenced by the instabilities and feedbacks discussed here, and other processes that remain underobserved, or unknown altogether. Projected rapid ice loss would partially offset global warming (*200*) by converting the heat into ice melt but would still cause SLR and alter ocean circulation as a result of the cooling and freshening of the oceans.

Uncertainty remains over how much Antarctica will warm within the Paris Agreement's 1.5°C target, owing to climate model uncertainties and potential polar amplification, which could cause Antarctica to warm sooner and exceed the global average. Even without the expected amplified warming, a global target of 1.5°C may not prevent the AIS from crossing tipping points within decades (*9*). The response timescale of the AIS is deeply uncertain, but its future contribution to SLR (Fig. 1B) could substantially exceed the IPCC medium-confidence projections within the next decades to century (*2*, *5*).

Summary and outlook

Antarctica stores a vast amount of freshwater, and its future evolution is the largest cause of uncertainty in SLR projections. Most of this uncertainty stems from insufficient understanding of key processes that affect the marginal ice shelves that buttress the ice sheet and the response of grounded ice when ice shelves are lost. Present observations are insufficient, in both space and time, to constrain the mechanisms responsible for abrupt mass loss, leaving them only crudely represented or missing entirely from ice sheet models. The impact of seasonal to decadal variations in climate forcing is also uncertain. Constraining the uncertainty in AIS evolution requires radically improved understanding of its mass-loss processes. Adequate sampling and tracking of changes can only be achieved through cooperative, new, and sustained observations from satellites and in situ observations (both on ice and in the surrounding ocean), combined with high-fidelity modeling to investigate key processes related to ice-ocean interactions, surface melting, and fracture of ice (Box 1).

Sir Douglas Mawson's words about his 1914 Antarctic expedition, "We had come to probe its mystery, we had hoped to reduce it to terms of science, but there was always the 'indefinable' which held aloof, yet riveted our souls," remain relevant in 2025. Our comprehension may always be incomplete, leaving open the likelihood that Antarctica's complexities surpass our capacity for complete understanding. However, societies need to understand Antarctica to be able to adapt in response to its changes. Yet despite this dire need and deep uncertainty, the pace of progress remains too slow, underscoring the need for a fundamental shift in our approach to polar science as we begin to identify and understand the once-indefinable unknowns. As we approach the Fifth International Polar Year (2031–2033), present limitations in observations and models highlight that polar science remains underequipped to fully address the complexities of Antarctica's system. We are at a time when a substantial increase in resourcing is needed to provide transformative advancements in research tools, data collection, and modeling capabilities, which are essential to unravel the key processes that shape the evolution of Earth's largest freshwater reservoir and to finally answer the critical questions: How much and how fast?

REFERENCES AND NOTES

1. M. Morlighem *et al.*, *Nat. Geosci.* **13**, 132–137 (2020).
2. B. Fox-Kemper *et al.*, in *Climate Change 2021: The Physical Science Basis. Contribution of Working Group I to the Sixth*

Assessment Report of the Intergovernmental Panel on Climate Change, V. Masson-Delmotte *et al.*, Eds. (Cambridge Univ. Press, 2021), pp. 1211–1362.
3. I. N. Otosaka *et al.*, *Earth Syst. Sci. Data* **15**, 1597–1616 (2023).
4. E. Rignot *et al.*, *Proc. Natl. Acad. Sci. U.S.A.* **116**, 1095–1103 (2019).
5. M. Oppenheimer *et al.*, in *The Ocean and Cryosphere in a Changing Climate: Special Report of the Intergovernmental Panel on Climate Change*, H.-O. Pörtner *et al.*, Eds. (Cambridge Univ. Press, 2019), pp. 321–445.
6. H. Seroussi *et al.*, *Earths Futur.* **12**, e2024EF004561 (2024).
7. S. Sadai, R. A. Spector, R. DeConto, N. Gomez, *Earths Futur.* **10**, e2022EF002940 (2022).
8. B. K. Galton-Fenzi *et al.*, in *Antarctica and Planet Earth*, M. Meredith, J. Melbourne-Thomas, M. Raphael, A. Naveira Garabato, Eds. (Taylor and Francis Group, 2024), chap. 7.
9. D. I. Armstrong McKay *et al.*, *Science* **377**, eabn7950 (2022).
10. N. S. Diffenbaugh, E. A. Barnes, *Proc. Natl. Acad. Sci. U.S.A.* **120**, e2207183120 (2023).
11. C. R. Stokes *et al.*, *Nature* **608**, 275–286 (2022).
12. J. E. Tierney *et al.*, *Science* **370**, eaay3701 (2020).
13. A. A. Robel, H. Seroussi, G. H. Roe, *Proc. Natl. Acad. Sci. U.S.A.* **116**, 14887–14892 (2019).
14. D. Li, R. M. DeConto, D. Pollard, *Sci. Adv.* **9**, eadd7082 (2023).
15. F. Pattyn, M. Morlighem, *Science* **367**, 1331–1335 (2020).
16. C.-Y. Tsai, C. E. Forest, D. Pollard, *Clim. Dyn.* **55**, 1875–1892 (2020).
17. L. G. Bennetts *et al.*, *Rev. Geophys.* **62**, e2022RG000781 (2024).
18. R. S. W. van de Wal *et al.*, *Earths Future* **10**, EF002751 (2022).
19. O. Gagliardini, G. Durand, T. Zwinger, R. C. A. Hindmarsh, E. Le Meur, *Geophys. Res. Lett.* **37**, L14501 (2010).
20. J. L. Bamber, M. Oppenheimer, R. E. Kopp, W. P. Aspinall, R. M. Cooke, *Earths Future* **10**, EF002772 (2022).
21. Intergovernmental Panel on Climate Change (IPCC), *Climate Change 2023: Synthesis Report. Contribution of Working Groups I, II and III to the Sixth Assessment Report of the Intergovernmental Panel on Climate Change*, Core Writing Team, H. Lee, J. Romero, Eds. (IPCC, 2023).
22. K. von Schuckmann *et al.*, *Earth Syst. Sci. Data* **15**, 1675–1709 (2023).
23. R. Mottram *et al.*, *Cryosphere* **15**, 3751–3784 (2021).
24. C. R. Stokes, *Earth Surf. Process. Landf.* **43**, 85–123 (2018).
25. C. Dow, N. Ross, H. Jeofry, K. Siu, M. Siegert, *Nat. Geosci.* **15**, 892–898 (2022).
26. F. Pattyn, *Earth Planet. Sci. Lett.* **295**, 451–461 (2010).
27. H. J. Zwally *et al.*, *Science* **297**, 218–222 (2002).
28. K. Boxall, F. D. W. Christie, I. C. Willis, J. Wuite, T. Nagler, *Cryosphere* **16**, 3907–3932 (2022).
29. B. J. Wallis, A. E. Hogg, J. M. Van Wessem, B. J. Davison, M. R. Van Den Broeke, *Nat. Geosci.* **16**, 231–237 (2023).
30. L. D. Trusel *et al.*, *Nat. Geosci.* **8**, 927–932 (2015).
31. R. L. Dell, I. C. Willis, N. S. Arnold, A. F. Banwell, S. De Roda Husman, *Nat. Geosci.* **17**, 624–630 (2024).
32. G. A. Jones *et al.*, *Geophys. Res. Lett.* **50**, e2023GL103673 (2023).
33. S. Sun *et al.*, *J. Glaciol.* **66**, 891–904 (2020).
34. D. J. Wingham, M. J. Siegert, A. Shepherd, A. S. Muir, *Nature* **440**, 1033–1036 (2006).
35. H. A. Fricker, T. Scambos, R. Bindschadler, L. Padman, *Science* **315**, 1544–1548 (2007).
36. S. J. Livingstone *et al.*, *Nat. Rev. Earth Environ.* **3**, 106–124 (2022).
37. L. A. Stearns, B. E. Smith, G. S. Hamilton, *Nat. Geosci.* **1**, 827–831 (2008).
38. T. A. Scambos, E. Berthier, C. A. Shuman, *Ann. Glaciol.* **52**, 74–82 (2011).
39. M. R. Siegfried, H. A. Fricker, S. P. Carter, S. Tulaczyk, *Geophys. Res. Lett.* **43**, 2640–2648 (2016).
40. B. I. D. Freer *et al.*, *J. Geophys. Res. Earth Surf.* **129**, e2024JF007724 (2024).
41. F. S. McCormack *et al.*, *Cryosphere* **17**, 4549–4569 (2023).
42. C. D. Gustafson *et al.*, *Science* **376**, 640–644 (2022).
43. A. A. Robel, S. J. Sim, C. Meyer, M. R. Siegfried, C. D. Gustafson, *Sci. Adv.* **9**, eadh3693 (2023).
44. E. Kazmierczak, S. Sun, V. Coulon, F. Pattyn, *Cryosphere* **16**, 4537–4552 (2022).
45. E. Kazmierczak, T. Gregov, V. Coulon, F. Pattyn, *Cryosphere* **18**, 5887–5911 (2024).
46. G. H. Gudmundsson, F. S. Paolo, S. Adusumilli, H. A. Fricker, *Geophys. Res. Lett.* **46**, 13903–13909 (2019).
47. J. J. Fürst *et al.*, *Nat. Clim. Chang.* **6**, 479–482 (2016).
48. B. Smith *et al.*, *Science* **368**, 1239–1242 (2020).
49. R. Reese, G. H. Gudmundsson, A. Levermann, R. Winkelmann, *Nat. Clim. Chang.* **8**, 53–57 (2018).
50. C. T. Wild *et al.*, *Cryosphere* **16**, 397–417 (2022).
51. B. W. J. Miles, R. G. Bingham, *Nature* **626**, 785–791 (2024).
52. M. Braun, A. Humbert, A. Moll, *Cryosphere* **3**, 41–56 (2009).
53. S. Lhermitte *et al.*, *Proc. Natl. Acad. Sci. U.S.A.* **117**, 24735–24741 (2020).
54. F. S. Paolo, H. A. Fricker, L. Padman, *Science* **348**, 327–331 (2015).
55. C. C. Walker *et al.*, *Nat. Geosci.* **17**, 1240–1248 (2024).
56. T. Scambos, C. Hulbe, M. Fahnestock, in *Antarctic Peninsula Climate Variability: Historical and Paleoenvironmental Perspectives*, E. Domack *et al.*, Eds., Antarctic Research Series, vol. 79 (American Geophysical Union, 2003), pp. 79–92.
57. M. S. Dinniman *et al.*, *Oceanography* **29**, 144–153 (2016).
58. I. Vaňková *et al.*, *Geophys. Res. Lett.* **50**, e2023GL102960 (2023).
59. M. G. Rosevear, B. Gayen, C. A. Vreugdenhil, B. K. Galton-Fenzi, *Annu. Rev. Mar. Sci.* **16**, 1–30 (2024).
60. A. K. Wåhlin *et al.*, *Sci. Adv.* **7**, eabd7254 (2021).
61. B. E. Schmidt *et al.*, *Nature* **614**, 471–478 (2023).
62. A. Dinh, E. Rignot, M. Mazloff, I. Fenty, *Geophys. Res. Lett.* **51**, e2024GL110078 (2024).
63. S. Adusumilli, H. A. Fricker, B. Medley, L. Padman, M. R. Siegfried, *Nat. Geosci.* **13**, 616–620 (2020).
64. B. K. Galton-Fenzi, J. R. Hunter, R. Coleman, S. J. Marsland, R. C. Warner, *J. Geophys. Res.* **117**, 2012JC008214 (2012).
65. B. Kulessa, D. Jansen, A. J. Luckman, E. C. King, P. R. Sammonds, *Nat. Commun.* **5**, 3707 (2014).
66. K. Lindbäck *et al.*, *Cryosphere* **13**, 2579–2595 (2019).
67. C. L. Stewart, P. Christoffersen, K. W. Nicholls, M. J. M. Williams, J. A. Dowdeswell, *Nat. Geosci.* **12**, 435–440 (2019).
68. K. A. Naughten *et al.*, *J. Clim.* **31**, 5243–5261 (2018).
69. D. E. Gwyther, C. F. Dow, S. Jendersie, N. Gourmelen, B. K. Galton-Fenzi, *Geophys. Res. Lett.* **50**, e2023GL103765 (2023).
70. A. Wåhlin *et al.*, *Sci. Adv.* **10**, eadn9188 (2024).
71. K. W. Nicholls *et al.*, *J. Glaciol.* **61**, 1079–1087 (2015).
72. I. Vaňková, K. W. Nicholls, H. F. J. Corr, K. Makinson, P. V. Brennan, *J. Geophys. Res. Earth Surf.* **125**, e2019JF005280 (2020).
73. S. Cook, K. W. Nicholls, I. Vaňková, S. S. Thompson, B. K. Galton-Fenzi, *Ann. Glaciol.* **63**, 27–32 (2022).
74. A. M. Chartrand, I. M. Howat, *J. Glaciol.* **69**, 1663–1676 (2023).
75. P. Milillo *et al.*, *Nat. Geosci.* **15**, 48–53 (2022).
76. P. Milillo *et al.*, *Sci. Adv.* **5**, eaau3433 (2019).
77. H. Chen, E. Rignot, B. Scheuchl, S. Ehrenfeucht, *Geophys. Res. Lett.* **50**, e2022GL102430 (2023).
78. E. Rignot *et al.*, *Proc. Natl. Acad. Sci. U.S.A.* **121**, e2404766121 (2024).
79. B. I. D. Freer, O. J. Marsh, A. E. Hogg, H. A. Fricker, L. Padman, *Cryosphere* **17**, 4079–4101 (2023).
80. E. Rignot, *Nat. Clim. Chang.* **13**, 1010–1013 (2023).
81. E. Rignot, J. Mouginot, M. Morlighem, H. Seroussi, B. Scheuchl, *Geophys. Res. Lett.* **41**, 3502–3509 (2014).
82. T. Pelle, J. S. Greenbaum, C. F. Dow, A. Jenkins, M. Morlighem, *Sci. Adv.* **9**, eadi9014 (2023).
83. T. Pelle, J. S. Greenbaum, S. Ehrenfeucht, C. F. Dow, F. S. McCormack, *J. Geophys. Res. Earth Surf.* **129**, e2023JF007513 (2024).
84. E. A. Wilson, A. J. Wells, I. J. Hewitt, C. Cenedese, *J. Fluid Mech.* **895**, A20 (2020).
85. A. A. Robel, E. Wilson, H. Seroussi, *Cryosphere* **16**, 451–469 (2022).
86. B. R. Parizek *et al.*, *J. Geophys. Res. Earth Surf.* **118**, 638–655 (2013).
87. R. T. Walker *et al.*, *Earth Planet. Sci. Lett.* **361**, 422–428 (2013).
88. H. Seroussi, M. Morlighem, *Cryosphere* **12**, 3085–3096 (2018).
89. A. T. Bradley, I. J. Hewitt, *Nat. Geosci.* **17**, 631–637 (2024).
90. Y. Wang *et al.*, *Cryosphere* **18**, 5117–5137 (2024).
91. K. Christianson *et al.*, *Geophys. Res. Lett.* **40**, 5406–5411 (2013).
92. L. M. Simkins, S. L. Greenwood, J. B. Anderson, *Cryosphere* **12**, 2707–2726 (2018).
93. C. L. Batchelor, J. A. Dowdeswell, *Mar. Geol.* **363**, 65–92 (2015).
94. R. B. Alley, S. Anandakrishnan, T. K. Dupont, B. R. Parizek, D. Pollard, *Science* **315**, 1838–1841 (2007).
95. A. G. C. Graham *et al.*, *Nat. Geosci.* **15**, 706–713 (2022).
96. C. L. Batchelor *et al.*, *Nature* **617**, 105–110 (2023).
97. M. Jakobsson *et al.*, *Geology* **39**, 691–694 (2011).
98. C. L. Parkinson, D. J. Cavalieri, *Cryosphere* **6**, 871–880 (2012).
99. D. K. Perovich *et al.*, *Geophys. Res. Lett.* **34**, 2007GL031480 (2007).
100. S. E. Stammerjohn, D. G. Martinson, R. C. Smith, X. Yuan, D. Rind, *J. Geophys. Res. Oceans* **113**, C03S90 (2008).
101. C. A. Greene, D. A. Young, D. E. Gwyther, B. K. Galton-Fenzi, D. D. Blankenship, *Cryosphere* **12**, 2869–2882 (2018).
102. M. Haigh, P. R. Holland, *Geophys. Res. Lett.* **51**, e2024GL108406 (2024).
103. A. Silvano *et al.*, *Sci. Adv.* **4**, eaap9467 (2018).
104. N. S. Steiner *et al.*, *Elementa* **9**, 00007 (2021).
105. A. Purich, E. W. Doddridge, *Commun. Earth Environ.* **4**, 314 (2023).
106. P. A. Reid, R. A. Massom, *Nat. Commun.* **13**, 1164 (2022).
107. E. Gilbert, C. Holmes, *Weather* **79**, 46–51 (2024).
108. S. Aoki *et al.*, *Commun. Earth Environ.* **3**, 142 (2022).
109. A. Duspayev, M. G. Flanner, A. Riihelä, *Geophys. Res. Lett.* **51**, e2024GL109608 (2024).
110. O. Schofield *et al.*, *Trends Ecol. Evol.* **39**, 1141–1153 (2024).
111. S. Kacimi, R. Kwok, *Cryosphere* **14**, 4453–4474 (2020).
112. M. Ionita, *Front. Earth Sci.* **12**, 1333706 (2024).
113. J. Weertman, *J. Glaciol.* **13**, 3–11 (1974).
114. C. Schoof, *J. Fluid Mech.* **573**, 27–55 (2007).
115. I. Joughin, B. E. Smith, B. Medley, *Science* **344**, 735–738 (2014).
116. E. A. Hill *et al.*, *Cryosphere* **17**, 3739–3759 (2023).
117. R. Reese *et al.*, *Cryosphere* **17**, 3761–3783 (2023).
118. M. Mengel, A. Levermann, *Nat. Clim. Chang.* **4**, 451–455 (2014).
119. T. Pelle, M. Morlighem, F. S. McCormack, *Geophys. Res. Lett.* **47**, e2019GL086821 (2020).
120. J. N. Bassis, C. C. Walker, *Proc. R Soc. A* **468**, 913–931 (2011).
121. R. M. DeConto, D. Pollard, *Nature* **531**, 591–597 (2016).
122. C. Needell, N. Holschuh, *Geophys. Res. Lett.* **50**, e2022GL102400 (2023).
123. I. Joughin, D. E. Shean, B. E. Smith, D. Floricioiu, *Cryosphere* **14**, 211–227 (2020).
124. M. G. Wise, J. A. Dowdeswell, M. Jakobsson, R. D. Larter, *Nature* **550**, 506–510 (2017).
125. T. L. Edwards *et al.*, *Nature* **566**, 58–64 (2019).
126. F. Clerc, B. Minchew, M. Behn, *Geophys. Res. Lett.* **46**, 12108–12116 (2019).
127. J. N. Bassis, B. Berg, A. J. Crawford, D. I. Benn, *Science* **372**, 1342–1344 (2021).
128. M. Morlighem *et al.*, *Sci. Adv.* **10**, eado7794 (2024).
129. R. B. Alley *et al.*, *Annu. Rev. Earth Planet. Sci.* **51**, 189–215 (2023).
130. J. N. Bassis *et al.*, *Annu. Rev. Earth Planet. Sci.* **52**, 221–247 (2024).
131. B. R. Parizek *et al.*, *Geology* **47**, 449–452 (2019).
132. A. J. Crawford *et al.*, *Nat. Commun.* **12**, 2701 (2021).
133. A. T. Bradley, D. T. Bett, P. Dutrieux, J. De Rydt, P. R. Holland, *J. Geophys. Res. Oceans* **127**, e2022JC018621 (2022).
134. M. Poinelli, Y. Nakayama, E. Larour, M. Vizcaino, R. Riva, *Geophys. Res. Lett.* **50**, e2023GL104588 (2023).
135. K. E. Alley, T. A. Scambos, R. B. Alley, *Ann. Glaciol.* **63**, 18–22 (2022).
136. C.-Y. Lai *et al.*, *Nature* **584**, 574–578 (2020).
137. J. A. MacGregor, G. A. Catania, M. S. Markowski, A. G. Andrews, *J. Glaciol.* **58**, 458–466 (2012).
138. S. Wang *et al.*, *J. Geophys. Res. Earth Surf.* **127**, e2021JF006346 (2022).
139. I. Joughin, D. Shapero, B. Smith, P. Dutrieux, M. Barham, *Sci. Adv.* **7**, eabg3080 (2021).
140. N. Gomez *et al.*, *Sci. Adv.* **10**, eadn1470 (2024).
141. V. R. Barletta *et al.*, *Science* **360**, 1335–1339 (2018).
142. P. St-Laurent, S. E. Stammerjohn, T. Maksym, *J. Geophys. Res. Oceans* **129**, e2023JC020467 (2024).
143. T. Surawy-Stepney *et al.*, *Cryosphere* **18**, 977–993 (2024).
144. R. A. Massom *et al.*, *Nature* **558**, 383–389 (2018).
145. N. J. Teder, L. G. Bennetts, P. A. Reid, R. A. Massom, *Environ. Res. Lett.* **17**, 045026 (2022).
146. K. Brunt, E. Okal, D. MacAyeal, *J. Glaciol.* **57**, 785–788 (2011).
147. C. C. Walker, J. N. Bassis, H. A. Fricker, R. J. Czerwinski, *J. Geophys. Res. Earth Surf.* **118**, 2354–2364 (2013).
148. M. K. Becker *et al.*, *Geophys. Res. Lett.* **48**, e2020GL091207 (2021).
149. C. A. Greene, A. S. Gardner, N.-J. Schlegel, A. D. Fraser, *Nature* **609**, 948–953 (2022).
150. A. D. Fraser *et al.*, *Rev. Geophys.* **61**, e2022RG000770 (2023).
151. G. Van Achter *et al.*, *Ocean Model.* **169**, 101920 (2022).
152. E. A. Cougnon *et al.*, *Geophys. Res. Lett.* **44**, 11519–11527 (2017).
153. M. F. Huguenin, R. M. Holmes, P. Spence, M. H. England, *Geophys. Res. Lett.* **51**, e2023GL104518 (2024).
154. R. J. Matear, T. J. O'Kane, J. S. Risbey, M. Chamberlain, *Nat. Commun.* **6**, 8656 (2015).
155. J. M. A. Macha *et al.*, *Geophys. Res. Lett.* **51**, e2024GL109423 (2024).
156. F. S. Paolo *et al.*, *Nat. Geosci.* **11**, 121–126 (2018).
157. M. A. King, P. Christoffersen, *Geophys. Res. Lett.* **51**, e2024GL108844 (2024).
158. H. H. Hellmer, F. Kauker, R. Timmermann, T. Hattermann, *J. Clim.* **30**, 4337–4350 (2017).
159. J. Jin, A. J. Payne, C. Y. S. Bull, EGUsphere egusphere-2024-1287 [Preprint] (2024); https://doi.org/10.5194/egusphere-2024-1287.
160. K. A. Naughten *et al.*, *Nat. Commun.* **12**, 1991 (2021).
161. B. J. Wallis *et al.*, *Nat. Commun.* **14**, 7535 (2023).
162. A. Shepherd, H. A. Fricker, S. L. Farrell, *Nature* **558**, 223–232 (2018).
163. T. Slater *et al.*, *Cryosphere* **15**, 233–246 (2021).
164. V. Brancato *et al.*, *Geophys. Res. Lett.* **47**, e2019GL086291 (2020).
165. B. W. J. Miles, C. R. Stokes, S. S. R. Jamieson, *Cryosphere* **12**, 3123–3136 (2018).
166. H. J. Picton, C. R. Stokes, S. S. R. Jamieson, D. Floricioiu, L. Krieger, *Cryosphere* **17**, 3593–3616 (2023).
167. S. S. Thompson *et al.*, *Cryosphere* **17**, 157–174 (2023).
168. R. Li *et al.*, *Nat. Commun.* **14**, 4061 (2023).
169. B. W. J. Miles *et al.*, *Cryosphere* **15**, 663–676 (2021).
170. B. J. Davison *et al.*, *Nat. Commun.* **14**, 1479 (2023).
171. S. Adusumilli, M. A. Fish, H. A. Fricker, B. Medley, *Geophys. Res. Lett.* **48**, e2020GL091076 (2021).
172. L. Barthélemy, F. Codron, V. Favier, J. Wille, Authorea 171387374.47240076/v1 [Preprint] (2024); https://doi.org/10.22541/au.171387374.47240076/v1.
173. S. Adusumilli, H. A. Fricker, A. S. Gardner, in *State of the Climate in 2022: Antarctica and the Southern Ocean*, K. R. Clem, M. N. Raphael, Eds. (American Meteorological Society, 2023).
174. J. D. Wille *et al.*, *J. Clim.* **37**, 757–778 (2024).
175. S. Jeong, I. M. Howat, J. N. Bassis, *Geophys. Res. Lett.* **43**, 11,720–11,725 (2016).

176. B. W. J. Miles *et al*., *J. Glaciol.* **66**, 485–495 (2020).
177. K. E. Alley *et al*., *Cryosphere* **15**, 5187–5203 (2021).
178. J. N. Bassis, H. A. Fricker, R. Coleman, J. B. Minster, *J. Glaciol.* **54**, 17–27 (2008).
179. C. C. Walker, J. N. Bassis, H. A. Fricker, R. J. Czerwinski, *J. Glaciol.* **61**, 243–252 (2015).
180. B. P. Lipovsky, *J. Geophys. Res. Oceans* **123**, 4014–4033 (2018).
181. D. Francis, K. S. Mattingly, S. Lhermitte, M. Temimi, P. Heil, *Cryosphere* **15**, 2147–2165 (2021).
182. E. Larour, E. Rignot, M. Poinelli, B. Scheuchl, *Proc. Natl. Acad. Sci. U.S.A.* **118**, e2105080118 (2021).
183. H. Seroussi *et al*., *Geophys. Res. Lett.* **44**, 6191–6199 (2017).
184. D. I. Benn *et al*., *Cryosphere* **16**, 2545–2564 (2022).
185. E. Rignot, *Philos. Trans. R. Soc. Ser. A* **364**, 1637–1655 (2006).
186. B. W. J. Miles, C. R. Stokes, S. S. R. Jamieson, *Sci. Adv.* **2**, e1501350 (2016).
187. T. Li, G. J. Dawson, S. J. Chuter, J. L. Bamber, *Cryosphere* **17**, 1003–1022 (2023).
188. N. Ribeiro *et al*., *J. Geophys. Res. Oceans* **128**, e2023JC019882 (2023).
189. S. Cook, B. K. Galton-Fenzi, S. R. M. Ligtenberg, R. Coleman, *Cryosphere* **12**, 3853–3859 (2018).
190. R. Minunno, N. Andersson, G. M. Morrison, *Earth Sci. Rev.* **241**, 104431 (2023).
191. D. R. Macayeal, K. Mankoff, B. Minchew, J. Moore, M. Wolovick, Glacial climate intervention: A research vision, Version 2, U.S. Antarctic Program Data Center (USAP-DC) (2024); https://doi.org/10.15784/601797.
192. B. Keefer, M. Wolovick, J. C. Moore, *PNAS Nexus* **2**, pgad053 (2023).
193. A. Alevropoulos-Borrill, N. R. Golledge, S. L. Cornford, D. P. Lowry, M. Krapp, *Commun. Earth Environ.* **5**, 150 (2024).
194. Ö. Gürses, V. Kolatschek, Q. Wang, C. B. Rodehacke, *Cryosphere* **13**, 2317–2324 (2019).
195. M. Siegert *et al*., ResearchGate 10.13140/RG.2.2.13179.94246 [Preprint] (2024); https://doi.org/10.13140/RG.2.2.13179.94246.
196. A. K. Klose, V. Coulon, F. Pattyn, R. Winkelmann, *Cryosphere* **18**, 4463–4492 (2024).
197. K. A. Naughten, P. R. Holland, J. De Rydt, *Nat. Clim. Chang.* **13**, 1222–1228 (2023).
198. J. Garbe, T. Albrecht, A. Levermann, J. F. Donges, R. Winkelmann, *Nature* **585**, 538–544 (2020).
199. D. Li, R. M. DeConto, D. Pollard, Y. Hu, *Nat. Commun.* **15**, 5178 (2024).
200. S. Sadai, A. Condron, R. DeConto, D. Pollard, *Sci. Adv.* **6**, eaaz1169 (2020).
201. A. Shepherd *et al.*, Antarctic and Greenland Ice Sheet mass balance 1992-2020 for IPCC AR6, Version 1.0, UK Polar Data Centre, Natural Environment Research Council, UK Research and Innovation (2021); https://doi.org/10.5285/77B64C55-7166-4A06-9DEF-2E400398E452.
202. L. A. Magruder *et al*., *Nat. Rev. Earth Environ.* **5**, 120–136 (2024).
203. J. Kingslake, J. C. Ely, I. Das, R. E. Bell, *Nature* **544**, 349–352 (2017).
204. T. Hattermann, L. H. Smedsrud, O. A. Nøst, J. M. Lilly, B. K. Galton-Fenzi, *Ocean Model.* **82**, 28–44 (2014).

ACKNOWLEDGMENTS

We thank the World Climate Research Programme Climate and Cryosphere Project (CliC) for coordinating this special issue, the EDGE Science Team for inspiration, and two reviewers whose comments substantially improved this paper. **Funding:** This work was funded by Eric and Wendy Schmidt (H.A.F.), NASA Cryospheric Sciences grant 80NSSC23K0934 (H.A.F.), the Australian Government by the Antarctic Science Collaboration Initiative Program (ASCI000002) (B.K.G.-F.), the Australian Research Council Special Research Initiative, the Australian Centre for Excellence in Antarctic Science (SR200100008), NASA Cryospheric Sciences grant 80NSSC22K0380 (C.C.W.), NASA Physical Oceanography grant 80NSSC23K0356 (C.C.W.), the Natural Environment Research Council (NERC) Satellite Data in Environmental Science (SENSE) Centre for Doctoral Training (NE/T00939X/1) (B.I.D.F.), a Schmidt AI Postdoctoral Fellowship (B.I.D.F.), NASA Cryospheric Sciences grants 80NSSC21K0911 and 80NSSC24K1029 (L.P.), the National Science Foundation (2213875 and 2035080) (R.D.), and NASA Cryospheric Sciences grant 80NSSC22K1707 (R.D.). **Competing interests:** The authors declare that they have no competing interests.

Submitted 19 October 2024; accepted 3 January 2025
10.1126/science.adt9619